

## OXYGEN DIFFUSION IN $\text{YBa}_2\text{Cu}_3\text{O}_{7-x}$ ; AN IMPEDANCE SPECTROSCOPY STUDY

D.J. VISCHJAGER, P.J. VAN DER PUT, J. SCHRAM and J. SCHOONMAN

*Delft University of Technology, Laboratory of Inorganic Chemistry, Julianalaan 136, 2628 BL Delft, The Netherlands*

Received 10 April 1988; in revised version 18 April 1988

The ionic conductivity of  $\text{YBa}_2\text{Cu}_3\text{O}_{7-x}$  has been studied in the temperature range of 650 to 1085 K, using  $\text{Pt}(\text{O}_2)/\text{YSZ}$  electrodes, which are ionically reversible, and blocking for electronic charge carriers. A.c. and d.c. polarization studies in air reveal an ionic conductivity activation enthalpy of 1.51 eV. In the range of 775 to 890 K ionic transference numbers range from  $2 \times 10^{-7}$  to  $8 \times 10^{-8}$ . The enthalpy value is related to ionic conduction via oxide ion vacancies  $\text{V}_\text{O}'$ , and oxygen loss.

### INTRODUCTION

Since the discovery of the high-temperature ceramic superconductor  $\text{YBa}_2\text{Cu}_3\text{O}_{7-x}$ , oxygen stoichiometry and ordering have been the subject of thorough investigations.

Oxygen ions in the  $\text{CuO}$  layer common to the two barium containing cubes in the  $\text{YBa}_2\text{Cu}_3\text{O}_{7-x}$  structure are the most loosely bound. These are the oxygen ions which disorder first on heating. Order-disorder phenomena in the oxygen sublattice are accompanied by loss of oxygen [1]. These observations indicate the oxygen ions to be mobile. In fact, Schwartz et al. [2] have shown that the oxygen content of  $\text{YBa}_2\text{Cu}_3\text{O}_{7-x}$  is reduced at room temperature by electrochemical reduction in a propylene carbonate/tetrabutylammonium perchlorate electrolyte. O'Sullivan and Chang [3] have used a solid-state oxygen concentration cell comprising  $\text{YBa}_2\text{Cu}_3\text{O}_{7-x}$  and sputtered Au as electrodes, and yttria-stabilized zirconia (YSZ) as the solid electrolyte. Using this cell, it was possible to electrochemically drive oxygen into and out of

the  $\text{YBa}_2\text{Cu}_3\text{O}_{7-x}$  electrode. The diffusivity of oxygen in 94% dense  $\text{YBa}_2\text{Cu}_3\text{O}_{7-x}$  was estimated to be  $\sim 5 \times 10^{-8} \text{ cm}^2 \text{ s}^{-1}$  at 823 K.

The effect of loss of lattice oxygen on the electrical properties of  $\text{YBa}_2\text{Cu}_3\text{O}_{7-x}$  has been studied by Fiory et al. [4]. These authors demonstrate that this oxygen loss accounts for the sharp rise in electrical resistivity at  $T > 675 \text{ K}$ , since the increase of  $x$  with temperature causes the density of electronic states to decrease, and the elastic scattering rate due to oxygen vacancy disorder to increase. Similar observations were reported by Tu et al. [5]. They relate the resistivity increase, as measured in He as ambient, to effusion of oxygen. The rate of diffusion is assumed to be limited by reactions at the solid-gas interface. In these studies d.c. measurements are used with electrodes that are blocking to ionic currents, and ohmic for electronic charge carriers. Hence, the reported resistivity variations are to be related to the majority charge carriers in this oxide. To obtain the ionic conductivity in  $\text{YBa}_2\text{Cu}_3\text{O}_{7-x}$  a different type of electrode is required.

The occurrence of mixed ionic and electronic conductivity at elevated temperatures opens the possibility of utilizing the ceramic superconductors as electrodes in solid-state electrochemical devices, like sensors and solid oxide fuel cells (SOFC). The ceramic superconductors like  $YBa_2Cu_3O_{7-x}$  and  $La_{1.85}Ba_{0.15}CuO_4$  may replace for instance the current state-of-the-art electrode material  $La(Sr)MnO_3$  in SOFC reactors. Little is known about the behaviour of these materials under SOFC reactor conditions.

We have studied ionic transport in several ceramic superconductors using a solid-state electrochemical cell comprising ionically reversible  $Pt(O_2)/YSZ$  electrodes which are blocking for electronic charge carriers, and the ceramic superconductor as a mixed-conducting solid electrolyte. Both a.c. impedance and d.c. polarization measurements have been performed. In addition, materials compatibility has been investigated. In this paper we report the results for  $YBa_2Cu_3O_{7-x}$ .

## EXPERIMENTAL ASPECTS

### MATERIALS

Ceramic superconductors  $YBa_2Cu_3O_{7-x}$  have been prepared by solid-state reaction using as starting materials  $Y_2O_3$  (Ventron 99.99 %),  $CuO$  (Ventron), and  $BaCO_3$  (Merck 99 %). Appropriate amounts of the reactants were thoroughly mixed, and pressed into pellets (5 kbar), and subsequently fired at 1223 K for 16 hours in air. After grinding the pellets, and pressing new pellets these were sintered in oxygen at 1223 K for another 16 hours. The temperature was then lowered to 673 K, and the pellets were kept at this temperature for 12 hours in oxygen. X-ray diffraction revealed the materials to have the orthorhombic structure. The samples exhibited a Meissner effect, and the electrical resistivity was measured as a function of temperature from 85 to 105 K with four-point resistance measurements. The data are presented in Figure 1.

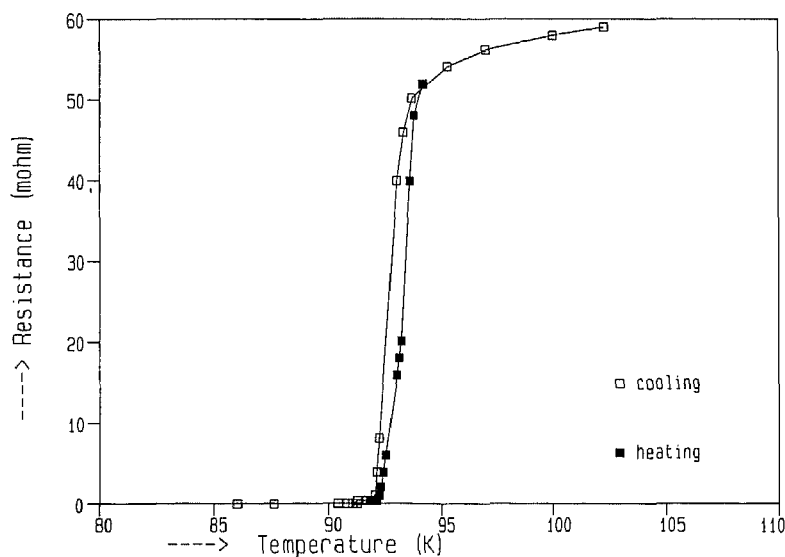


Figure 1 ; Superconducting transition in  $YBa_2Cu_3O_{7-x}$  as measured by the four-point resistance method

## IMPEDANCE SPECTROSCOPY

Two types of solid-state electrochemical cells have been studied: (1) Pt(air)/YSZ/Pt(air), and (2) Pt(air)/YSZ/ $YBa_2Cu_3O_{7-x}$ /YSZ/Pt(air).

YSZ (zirconia stabilized with 8 mole percent (m/o) yttria (Gimex)), was used in combination with Pt as an ion reversible electrode for the  $YBa_2Cu_3O_{7-x}$ .

The first cell served as a reference.

Disks, 1 mm to 2 mm thickness and 5 mm in diameter, of the YSZ solid electrolyte were provided with sputtered Pt electrodes (Edwards Sputter Coater, S150 B) on both sides of the YSZ disks for cell 1 and on one side of the YSZ disks for cell 2. The solid-state cells were springloaded between Pt disks in a nickel conductivity cell, which was provided with resistive heating. As ambients purified nitrogen, air, and oxygen were used. The small-signal a.c. response of the cells was recorded in the temperature range of 700 to 1100 K, using a computer-controlled Solartron 1250 Frequency Response Analyser, in combination with a

Solartron 1286 Electrochemical Interface.

Admittance spectra were measured in the frequency range 0.1 to 65,000 Hz. A complex non-linear least-squares method has been used to fit the measured frequency dispersions of the solid-state cells to an equivalent electrical circuit description. An integrated software package was used, involving coordinated data storage, graphical presentation, and a Marquardt non-linear least-squares parameter estimation for complex data.

In several instances, d.c. polarization experiments were performed on cell 2. The decay of the current was monitored with an autoranging Keithley 485 picoammeter. D.c. voltages in the range 0.1 to 0.2 V were applied.

## RESULTS

Cell 1

The low-frequency tail in the admittance spectra of the cells Pt/YSZ/Pt in nitrogen ambient extrapolate to zero conductance. In air and

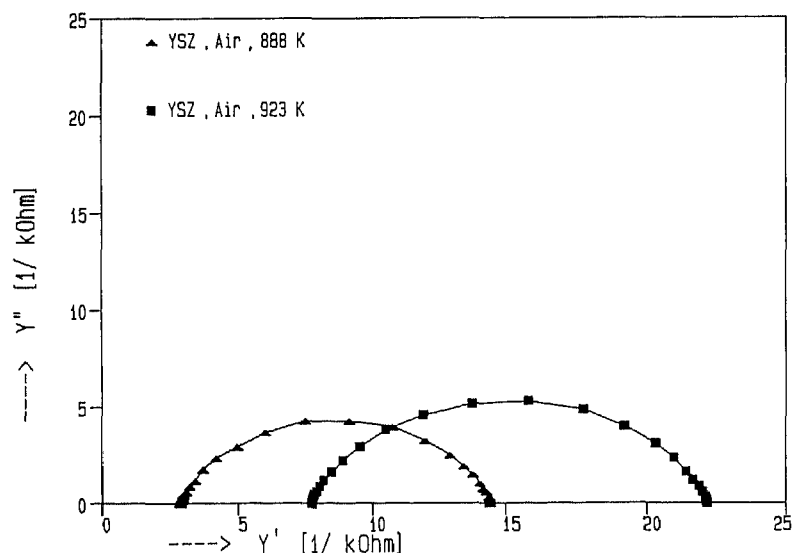
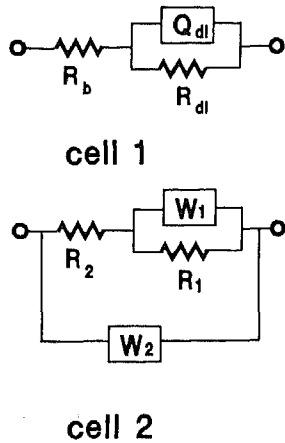


Figure 2 ; Admittance spectra of the cell Pt(air)/ $ZrO_2:Y_2O_3(8m/o)$ /Pt(air) at 888 and 923 K. Frequency range 0.1 to 65,000 Hz.



**Figure 3** ; Equivalent electrical circuits for cells 1 and 2. See text.

oxygen a d.c. conduction pathway is observed, indicating the  $\text{Pt}(\text{O}_2)$  electrodes to become partly ionically reversible. Representative admittance spectra are presented in Figure 2. In the accessible frequency range and the temperature range of 700 to 1000 K the admittance spectra can be modelled with an equivalent circuit  $R_{dl}Q_{dl} \parallel R_b$  s, where  $Q_{dl}$

represents a double layer constant-phase-element (CPE) with admittance  $Y_{Q_{dl}} = k_Q(i\omega)^\alpha$ ,  $R_{dl}$  a Faraday resistance, shunting the double layer CPE element.

$R_b$  represents the bulk resistance of  $\text{ZrO}_2: \text{Y}_2\text{O}_3$  (8 m/o), while s stands for series and p for parallel.  $R_{dl}$  decreases with increasing oxygen partial pressure as expected. In the studied temperature range of  $\alpha$  varies between 0.65 and 0.75. The equivalent circuit is presented in Figure 3, while  $R_b$  and  $R_{dl}$  data are presented in an Arrhenius plot of  $\sigma T$  vs  $1000/T$  in Figure 4.

#### Cell 2

The small signal a.c. response of  $\text{YBa}_2\text{Cu}_3\text{O}_{7-x}$  in between the partially oxygen reversible electrodes is presented in Figure 5. The response data could be fitted to the equivalent circuit  $R_1W_1 \parallel R_2$  s  $W_2$  p. The equivalent circuit is presented in Figure 3. Here W denotes a diffusional impedance with admittance  $Y_W = k_W(i\omega)^{1/2}$ . The  $R_1$  and  $R_2$  data are included in Figure 4. D.c. polarization experiments on cell 2 reveal

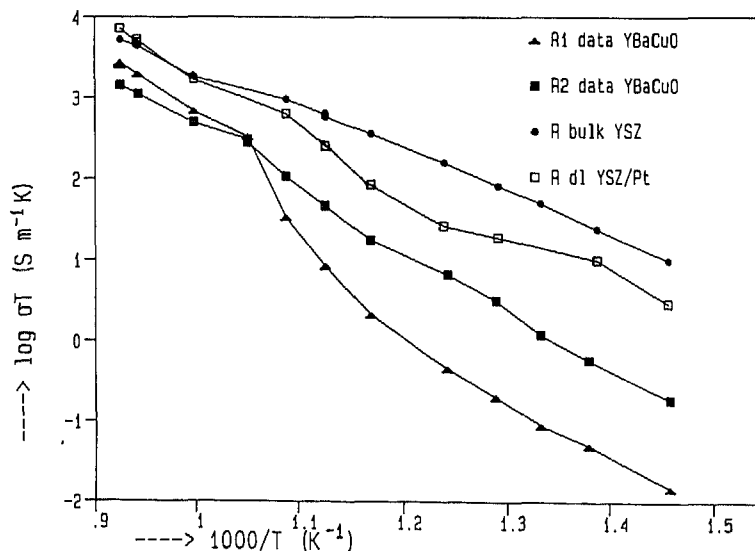


**Figure 4** ; Temperature dependence of the bulk ionic conductivity of  $\text{ZrO}_2: \text{Y}_2\text{O}_3$  (8 m/o), and of specific conductivities calculated from  $R_1$  and  $R_2$  data of  $\text{YBa}_2\text{Cu}_3\text{O}_{7-x}$ , plotted as  $\log \sigma T$  vs  $1000/T$ .

time dependent currents. In the temperature range of 773 to 898 K currents decay to stationary values over a period of 24 hours. Numerical data for the stationary currents are presented in Table 1, along with values for the equivalent circuit elements  $R_1$  and  $R_2$  (viz. Figure 3). From the polarization experiments the values 154 kOhm and 25 kOhm are calculated for the resistance of the polarized cell 2 at 778 and 882 K, respectively. Spectrum analyses of YSZ reveal  $R_b$  to be 1 kOhm at 774 K, and 160 Ohm at 889 K. At these temperatures  $R_{dl}$  has the

Table 1

Stationary currents  $i_s$  for cell 2 and numerical values for  $R_1$  and  $R_2$  as obtained from admittance data fitting.

T(K)	V(V)	$i_s$ ( $\mu$ A)	$R_1$ (kOhm)	$R_2$ (kOhm)
778	0.100	0.65		
776			218	14
882	0.100	4.0		
889			6	1

value 4.5 kOhm and 340 Ohm, respectively. Under all circumstances reported in this work neither degradation, nor solid-state reactions occur at the YSZ/ $YBa_2Cu_3O_{7-x}$  interfaces.

DISCUSSION

The admittance spectra of the cell Pt( $O_x$ )/YSZ/Pt( $O_x$ ) indicate a d.c. conduction pathway for which  $R_{dl}$  is responsible. The interface reaction  $1/2 O_2 (g) + V_{O}^{\bullet\bullet} + 2e' \rightleftharpoons O_O^x$ , in which the Kröger-Vink defect notation is used, describes the oxygen reversibility of the Pt( $O_x$ )/YSZ interface. The depressed semicircles may be associated to current inhomogeneities at the interface, due for instance to rough surfaces. A detailed analysis of the imaginary parts of the present spectra is beyond the scope of this paper.

Ideally, the equivalent circuit of cell 2 would be described by the equivalent circuit  $R_1 C_1 \parallel R_2 \parallel R_3 C_3$  in series with the equivalent circuit for cell 1, the latter circuit now representing both reversible

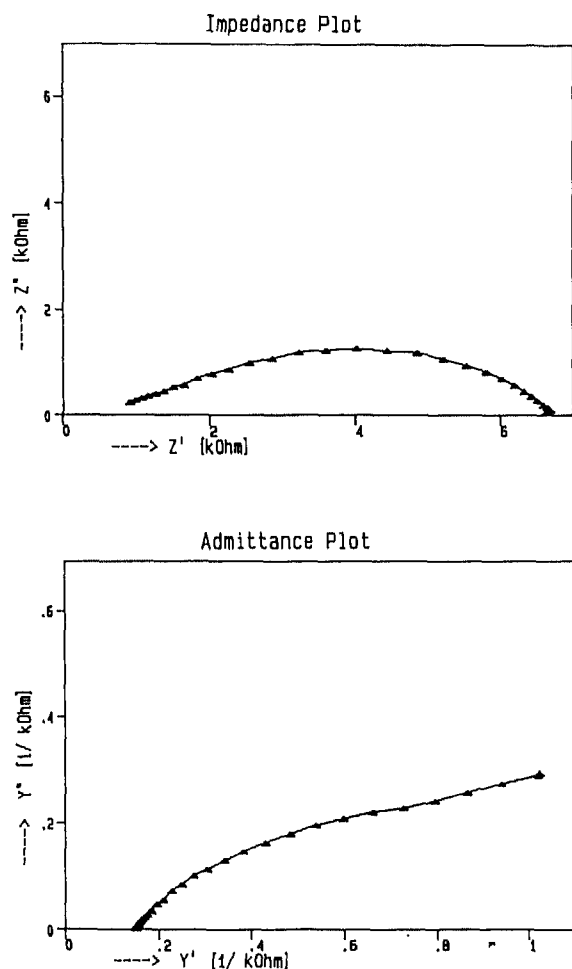


Figure 5 ; Admittance, and concomitant impedance spectrum of cell 2 in air at 880 K. Frequency range 0.1 to 65,000 Hz.

Pt(O<sub>2</sub>)/YSZ electrodes.  $R_2$  then stands for the bulk ionic conductivity of  $YBa_2Cu_3O_{7-x}$ , and  $R_1C_1$  p for a possible polarization effect of oxide ions at grain boundaries. The parallel branch, comprising  $R_3C_3$  s, is due to electronic charge carriers, the capacitance arising from the blocking of these electronic charge carriers at the  $YBa_2Cu_3O_{7-x}$ /YSZ interface. Of the resistive circuit elements,  $R_3$  has by far the smallest value. The equivalent circuit actually found to describe the small-signal a.c. response of cell 2 reveals that the relaxation times including  $R_1$  and  $R_2$  dominate the system response. We, therefore, attribute  $R_1$  to a grain boundary effect, and  $R_2$  to bulk ionic conductivity. The electronic conductivity of  $YBa_2Cu_3O_{7-x}$  exceeds the ionic conductivity by orders of magnitude. Hence,  $R_3$  does not show up in the fitting results. The response data further indicate that the interface ionic polarization phenomena at either grain boundaries in  $YBa_2Cu_3O_{7-x}$ , or at the  $YBa_2Cu_3O_{7-x}$ /YSZ interface are governed by diffusional processes. These are currently the subject of further investigations. The low-frequency data in Figure 5 reveal the d.c. conductance of cell 2 at 880 K in air to be  $1.4 \times 10^{-4}$  S. The reciprocal value represents the resistive d.c. path of cell 2, i.e.  $R_{dl} + R_b + R_1 + R_2$ . The ionic charge carriers in YSZ are the oxide ions, which migrate via the oxide ion vacancies  $V_O^{\bullet\bullet}$ . Marucco et al. [6] have concluded from a thermogravimetric study on  $YBa_2Cu_3O_{7-x}$  in controlled oxygen pressures, that in the orthorhombic phase fully ionized oxide ion vacancies,  $V_O^{\bullet\bullet}$ , are likely to be predominant. Hence the d.c. ionic conduction path in cell 2 is due to oxide ion migration via oxide ion vacancies  $V_O^{\bullet\bullet}$ . The numerical values for the resistive circuit elements indicate that  $R_{dl}$  and  $R_b$  of YSZ can be neglected at about 880 K. The stationary current data in Table 1 lead to a conductance value of  $4 \times 10^{-5}$  S, which is substantially lower than the

zero-frequency conductance. It should, however, be borne in mind that part of the applied d.c. voltage across cell 2 is compensated by the interfacial space charge effects as represented by  $Q_{dl}$ ,  $W_1$  and  $W_2$  (viz. Figure 3). The numerical values of  $R_1$  and  $R_2$  in Table 1 are used to calculate the voltage drop across  $YBa_2Cu_3O_{7-x}$ . For example at 889 K this voltage drop is about 28 mV, if we use the value  $4 \times 10^{-6}$  A for  $i_s$ , as obtained at 882 K. The voltage drop across the two YSZ electrodes is about 2 mV at 889 K. These voltage data clearly show, that a substantial part ( $\sim 70$  mV) of the applied d.c. voltage is stored in  $Q_{dl}$ ,  $W_1$  and  $W_2$ . From the Arrhenius curve of the  $R_2$  data in Figure 4 we calculate for the ionic conductivity activation enthalpy of  $YBa_2Cu_3O_{7-x}$  the value of 1.51 eV. The ionic conductivity data, and the literature data for the electronic conductivity of  $YBa_2Cu_3O_{7-x}$  in air [4] lead to ionic transference numbers ranging from  $2 \times 10^{-7}$  to  $8 \times 10^{-6}$  in the temperature range of 775 to 890 K. Haller et al. [7] have determined the activation energy for oxygen uptake to be 1.12 eV. This value is ascribed to oxide ion diffusion in  $YBa_2Cu_3O_{7-x}$ . Tu et al. [5] found 1.7 eV to be the activation energy for the interfacial-reaction limited effusion of oxygen. The present conductivity activation enthalpy value of 1.51 eV is found in between these two values, indicating that in addition to vacancy conduction loss of oxygen occurs. This is to be expected, if  $YBa_2Cu_3O_{7-x}$  is heated in air in the temperature range used in the present study. The Arrhenius plot of the  $R_1$  data for  $YBa_2Cu_3O_{7-x}$  reveals at moderate temperatures a conductivity activation enthalpy which is concordant to that for bulk ionic conduction. From about 890 K to 950 K an upward curvature is observed. Beyond 950 K  $R_1$  and  $R_2$  data reveal the same conductivity activation enthalpies. Although sintering effects will affect the grainboundary polarization phenomena, and hence resistance  $R_1$ ,

the resistivity and structural data reported by Fiory et al. [4] reveal  $YBa_2Cu_3O_{7-x}$  to transform in air into the tetragonal phase at about 895 K. Both sintering and structural transformation may, therefore, be the cause of the upward curvature in the Arrhenius plot of the  $R_1$  data. The present study clearly demonstrates the versatility of the use of ionically reversible electrodes in the study of the electrical properties of the ceramic superconductors with a.c. and d.c. methods.

We are currently using cell 2 to study ionic conduction in  $La_{1.8}Ba_{0.2}CuO_4$ ,  $La_{1.8}Sr_{0.2}CuO_4$ , and  $Bi_2Cu_2(Sr_{.56}Ca_{.39}Bi_{.05})_3O_{8-x}$ . Further work on the utilization of the ceramic superconductors as solid-state electrodes is in progress.

#### ACKNOWLEDGEMENTS

The authors are grateful to Mr. H. Vuurens for material synthesis, and Mr. R.W. Willekers for low temperature resistivity measurements. This study was supported in part (D.J.V.) by the Netherlands Organization for Applied Scientific Research (TNO).

#### REFERENCES

- [1] G. van Tendeloo, S. Amelinckx; Phys. Stat. Sol. (a) 103 (1987) K1.
- [2] M. Schwartz, M. Rappaport, G. Hodes and D. Cahen; Proc. Int. Conference on High Temperature Superconductors and Materials, and Mechanisms of Superconductivity, Interlaken, (1988) in press.
- [3] E.J.M. O'Sullivan, B.P. Chang; Appl. Phys. Letters, in press.
- [4] A.T. Fiory, M. Gurvitch, R.J. Cava, G.P. Espinosa; Phys. Rev. B 36 (1987) 7262.
- [5] K.N. Tu, S.I. Park, C.C. Tsuei; Appl. Phys. Letters 51 (1987) 2158.
- [6] J.F. Marucco, C. Noguera, P. Garoche, G. Collin; J. Mater. Res. 2, (1987) 757.
- [7] I. Haller, M.W. Shafer, R. Figat, D.B. Goland; Pure and Appl. Chem. in press, cited in ref. 3.